Hybridization methodology based on DP algorithm for hydraulic mobile machinery — Application to a middle size excavator

Elsevier Editorial System(tm) for Automation in Construction

Manuscript Draft

Manuscript Number: AUTCON-D-15-00107R2

Title: Hybridization Methodology based on DP algorithm for Hydraulic Mobile Machinery - Application to a Middle Size Excavator

Article Type: Original Paper

Keywords: Hydraulic Hybrid Excavator; Hybridization Methodology; Dynamic Programming Optimization

Corresponding Author: Prof. PAOLO CASOLI, Master

Corresponding Author's Institution: University of Parma

First Author: PAOLO CASOLI, Master

Order of Authors: PAOLO CASOLI, Master; Agostino Gambarotta, PhD; Luca Riccò, Master; Nicola Pompini, Master

HYBRIDIZATION METHODOLOGY BASED ON DP ALGORITHM FOR HYDRAULIC MOBILE MACHINERY – APPLICATION TO A MIDDLE SIZE EXCAVATOR

Casoli P., Gambarotta A., Pompini N., Riccò L.
Industrial Engineering Department, University of Parma Italy, Parco Area delle Scienze 181/A, 43124 Parma (PR) ITALY

Corresponding author: Paolo Casoli
paolo.casoli@unipr.it;
Industrial Engineering Department
University of Parma Italy
Parco Area delle Scienze 181/A
43124 Parma (PR) ITALY
Phone: +390521 905868
FAX: +39 0521 905705

Answer to Reviewers

II round

Editor:
In addition to the reviewers' comments below, please address the following:
- Highlights: the first one is too long.
- Figures: if at all possible (this may be the case for most of your figures), please submit images in vector format (i.e. where text is text and lines are lines, as opposed to everything being pixels). Examples of formats supporting vector content are PDF and EPS. MS Office files are also accepted by the journal (e.g. EMF).
- Conclusions: Your conclusions should include opening statements that review the limitations of the work reported in the manuscript and suggest areas for further research.

Answer: the first highlight has been corrected; figures has been prepared as required; conclusions have been improved as required, a sentence has been added at the end and little modifications at the beginning have been introduced.

Reviewer #2:
The authors have made substantial changes to this paper from their original submission. These changes have greatly improved the quality of this paper and it is now this reviewer's opinion that the paper be published in its current state.

The only minor suggestion, which if not addressed should not keep this paper from being published, is to include a zoomed-in view of Figure 30. This plot shows the command to a proportional valve but the time scale doesn't allow the reader to see if the valve is ever commanded to a position other than fully open or fully closed.

Answer: A figure has been added as required (fig. 31) . Figs. 30 and 33 have been little modified.

Reviewer #3:
Well written and well reworked. i have no further comments.

Answer: Thanks.

Highlights

1. A methodology to compare different hydraulic hybrid system layouts is presented.
2. The methodology takes advantage of the dynamic programming (DP) algorithm.
3. Optimal hybrid layout configuration and its optimal control policies can be defined

Hybridization Methodology based on DP algorithm for Hydraulic Mobile Machinery – Application to a Middle Size Excavator

Casoli P., Gambarotta A., Pompini N., Riccò L.

Industrial Engineering Department, University of Parma Italy, Parco Area delle Scienze 181/A, 43124 Parma (PR) ITALY

Corresponding author: Paolo Casoli
paolo.casoli@unipr.it;
Industrial Engineering Department
University of Parma Italy
Parco Area delle Scienze 181/A
43124 Parma (PR) ITALY
Phone: +390521 905868
FAX: +39 0521 905705

Abstract

Fuel consumption and pollutant emission reduction are and will continue to be the most important drivers in the improvement of mobile machinery hydraulic system. Many different solutions and options are proposed in the literature to improve the machinery fuel efficiency, and many of these are based on hybrid solutions. The aim of this paper is to present a hybridization methodology which allows to compare different system layouts, to dimension the energy storage devices, to define the optimal control policies, and finally to determine the more effective hybrid system layout. The proposed methodology takes advantage of the dynamic programming (DP) algorithm. The machinery mathematical model and information about working cycle have to be known "a priori" in order to take advantage of the presented methodology.

The hybridization methodology has been applied to a hydraulic excavator as a guideline example, and the results are reported in the last section of the paper.

Keywords: Hydraulic Hybrid Excavator; Hybridization Methodology; Dynamic Programming Optimization.

Nomenclature

Abbreviations

AUX	Auxiliary	VCO	Variable Control Orifice
DoE	Design of Experiment	ICE	Internal Combustion Engine
DP	Dynamic Programming	JCMAS	Japan Construction Machinery Association Standard
ECU	Electronic Control Unit	LS	Load Sensing

Symbol	Description	Unit	Symbol	Description	Unit
A_A	Hydraulic Actuator Piston Area	[m^2]	V	Volume	[m^3]
A_B	Hydraulic Actuator Piston Area	[m^2]	Vd	Volumetric Displacement	[m^3/r]
c_d	Discharge Coefficient	[-]	w	System Disturbance	
F	Force	[N]	x	System State	
J	Cost Function		x_i	Spool Linear Position	[m]
mf	Fuel Burned Rate	[g/s]	y	System Output	
n	Angular Velocity	[r/min]	γ	Polytropic Index	
p	Pressure	[Pa]	η_{hm}	Hydraulic-Mechanical Efficiency	[-]
Q	Volumetric Flow Rate	[m^3/s]	η_V	Volumetric Efficiency	[-]
T	Torque	[N·m]	π	Control Policy	
u	System Input		ρ	Hydraulic Density	[kg/m^3]
v	Linear Velocity	[m/s]	ω	Angular Velocity	[rad/s]

Superscript

*	Optimal

1. Introduction

In the field of mobile machinery the increasing interest in the reduction of pollutant emissions, supported by more and more tight regulations, and of fuel consumption are leading the R&D activities towards new energy saving solutions. Focusing on hydraulic mobile machinery, especially on hydraulic excavators, there are different options to reduce fuel consumption. A first way is the improvement of single components efficiency, achieved by reducing friction losses and/or enhancing their flow dynamics characteristics. A second path concerns the adoption of new system layouts, e.g., drive hydraulic actuators in closed loop hydraulic system using variable displacement machines (thus avoiding throttling losses in valves) [*1*], or adopting hydraulic transformers [*2*]. A further solution is the optimization of the matching between the internal combustion engine (ICE) and the hydraulic system taking account of the mission profile [*3, 4*]. Furthermore, new electro-hydraulic solutions are also under investigation, e.g., Electro Flow Matching (EFM) [*5*] and Electro Positive Control (EPC) [*6*]. Hybridization techniques, i.e., the use of two or more distinct power sources, combined with energy recovery systems, represent a further solution. Hybridization technology is widely used on on-road vehicles, where the ICE and an electric system (generator, motor, inverter and battery) are coupled, with

significant advantages in the improvement of fuel efficiency and pollutant emissions reduction, when optimized energy management strategies and a proper design of components and overall architecture are adopted [*7*].

Concerning hydraulic excavators, during a typical working cycle the required power and torque vary periodically in a wide range, influencing consequently the engine working conditions. Moreover, kinetic energy of the turret and gravitational energy of the boom are typically dissipated as heat in the flow control valves. Thus, hybrid excavators with energy recovery systems seem to be an effective solution to improve fuel efficiency, thanks to the possibility of a better shaping of the load request to the ICE and the storage of otherwise wasted energy.

Developing an optimized hybrid system involves several topics such as the system layout definition, components size specification and optimal energy management strategy definition. Many researchers have studied hybrid electric excavators focusing on the optimal control strategy definition of some proposed electric hybrid excavator layouts [*8, 9, 10, 11*]. As previously mentioned, during the typical working cycle of a hydraulic excavator the required power and torque change rapidly, periodically and in a very wide range. Furthermore, since boom and turret movements are very fast, a hydraulic energy recovery system seems better than electrical one for this specific application [*12*], thanks to its higher power density instead of a higher energy density.

The aim of this paper is to define a methodology to compare different proposed hybrid system layouts. The methodology has been applied to a middle size (9 t) excavator. For this machinery, four different hydraulic hybrid layouts were proposed and compared. For each layout it has been necessary to define both the new components required for the energy recovery and the optimal energy management strategy in order to achieve the best fuel economy.

The proposed methodology takes advantage of the dynamic programming (DP) algorithm [*13*] in order to define the optimal control policy (in this specific case minimizing fuel consumption) for the non-linear, time dependent problem of excavator dynamics during a defined typical working cycle. This powerful optimization technique has been used widely for defining optimal control strategy for hybrid on-road vehicles [*14*] and to investigate novel hydraulic hybrid architectures for on-road vehicles [*15*]. Using the DP algorithm for each considered/proposed layout it is possible to optimally size the components of interest through a DoE (Design of Experiment) procedure. Then it is finally possible to determine the hybrid layout which guarantees the lower fuel consumption after comparing all the studied layouts in their best energy saving configuration.

For applying the presented hybridization methodology some necessary steps have to be done:

- starting from the standard machinery mathematical model (with a direct causality), an inverse causality model has to be defined and validated. The direct causality model is also exploited to define the inputs required by the inverse model;

- a representative working cycle for the considered machine has to be defined; for hydraulic excavators, a typical working cycle has been identified in the JCMAS H020:2007 [*16*], where no interaction between bucket and ground is considered;
- different hybrid layouts have to be defined for the considered machinery as well as their inverse causality model;
- the optimization problem has to be formulated;
- finally the hybrid layouts can be compared in order to define the best energy saving solution.

The paper is organized as follows: section 2 presents the standard machinery hydraulic layout previously analyzed and modelled by the authors (assumed as reference for the current analysis), the standard machinery inverse modelling and its validation on the selected reference working cycle; section 3 describes the optimization problem definition and the dynamic programming algorithm; section 4 describes the proposed hydraulic hybrid layouts and their inverse causality model schemes, as well as the DoE performed for the optimal components sizing; section 5 shows the optimization results obtained applying the presented methodology.

2. Physical Modeling

2.1 Direct causality model

The machinery taken into account for this study is a middle size excavator whose simplified hydraulic circuit ISO scheme is reported in Fig.1. The hydraulic layout of this kind of machinery can be divided in three parts [*17*]: the generator section composed of the hydraulic pumps which transform the power output of the ICE into hydraulic power; the conductive section which transfers pressurized fluid to actuators via pipes and valves; the motor related section where fluid is used to move hydraulic cylinders, motors and auxiliaries.

The actuators considered in the mathematical model are those required for the defined working cycle [*16*]. As can be seen in Fig.1, the arm, boom and bucket cylinders and the turret (or swing) and travels motors have been considered, along with the related hydraulic flow control valves.

The main hydraulic circuit is a Load-Sensing (LS) system, where the highest load pressure level of parallel operating hydraulic drives is detected and fed back to the pump regulators and to the valves pressure compensators. This allows to control the inlet line pressure and keep a constant pressure drops across metering valves, even in flow saturation conditions.

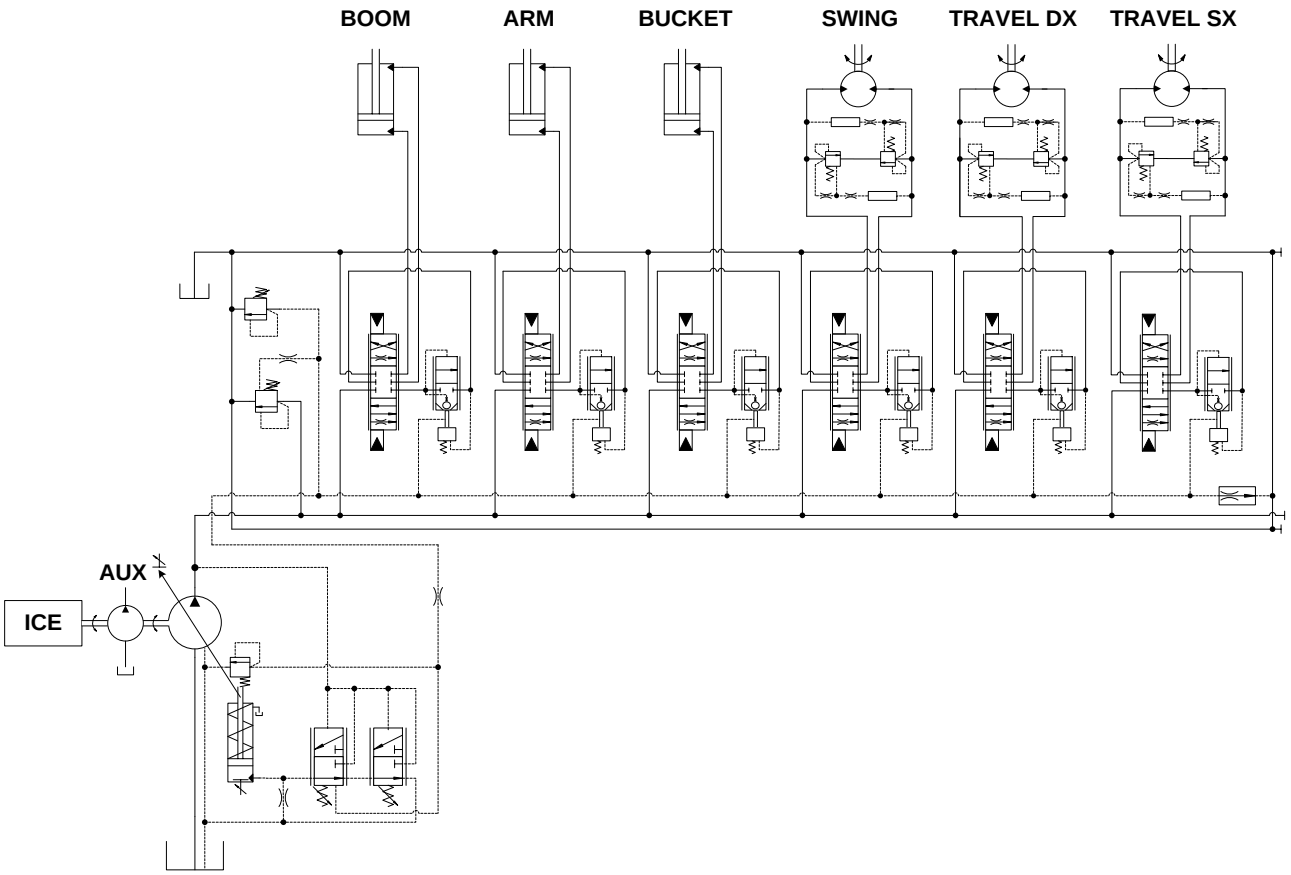

Fig. 1. ISO scheme of the standard excavator hydraulic circuit.

The main pump is a LS variable displacement axial piston pump and its mathematical model has been already developed and validated both in steady state and dynamic conditions [*18, 19*]. The main valve is a LS full flow sharing sectional valve. The valve block mathematical model has been already presented and validated with the comparison between numerical and experimental results [*20*]. The mathematical model considers also the front excavation tools, in order to reproduce the real forces acting on the hydraulic actuators during the implements movements. A detailed description of the standard machinery mathematical modelling is presented in [*21*]. The pilot circuit (AUX), powered by a fixed displacement external gear pump, operating at a constant pressure level, has been considered since it has a significant impact on the fuel consumption. The ICE is a Diesel engine and its mathematical model has been presented in [*22*]. The direct causality models are dynamic models based on differential equation. Pressures inside the chambers are calculated through the pressure rise rate equation applied to the chambers volume, the shaft speed is defined through the momentum equilibrium of the engine/pump shaft and forces acting on the hydraulic actuators are defined thought the second Newton's law applied to the moving bodies of the kinematics. Figure 2 reports the direct causality mathematical model scheme.

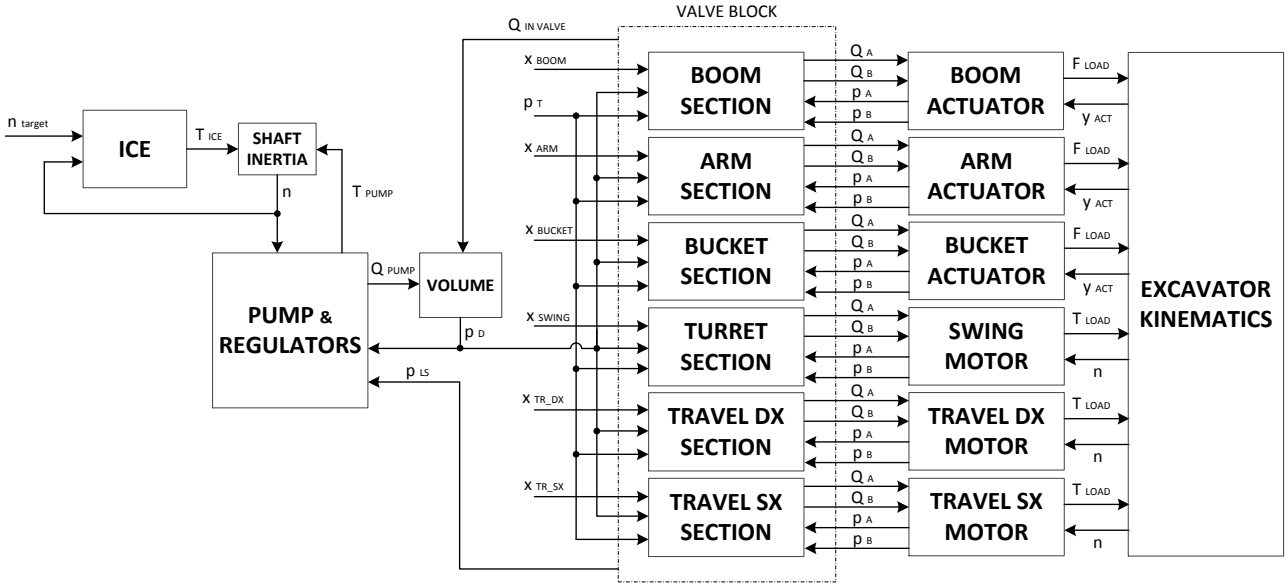

Fig. 2. Direct causality model of the standard excavator.

2.2 Inverse Causality Model

The presented optimization methodology, as previously mentioned, is based on the DP algorithm which has the characteristic of solving dynamic optimization problems backward-in-time. In order to solve the optimization problem the causality of the developed model has to be reverted. Due to the exponentially increasing complexity and computation time required to solve a DP problem with a large number of states (i.e. a model with many differential equations), all the non-essential dynamics of the model have been neglected. For this reason, when reversing the causality of the model, all sub-models have been reduced to pure algebraic models based on a Quasi-Steady formulation. This is justified by the fact that the time constants associated with the hydraulic components are very low compared to the characteristics time of a duty cycle. The comparison between excavator direct and inverse causality models presented in section 2.4 proves the validity of this assumption.

On the other hand, when introducing an energy recovery device, i.e. a hydraulic accumulator, it becomes clear that its dynamics cannot be neglected as they are considerably slower than the hydraulics one and greatly affects the behavior of the system.

Regarding the control of expander movements, in the direct causality case the forces applied to the moving parts depend on the inputs imposed by the driver (control valves positions) and the trajectories of the excavator components are calculated (i.e., boom, arm, bucket and swing); in this case, a driver model (namely a PI controller has been used to guarantee that the actual excavator tools trajectories match the desired profile set by the reference working cycle. In the

reverse causality case on the other hand, kinematics of the actuators are known a priori (being defined by the working cycle) and the forces acting on the actuators can be easily derived from the dynamic equilibrium equation.

2.2.1 Hydraulic Linear Actuator

Figure 3 shows the hydraulic linear actuator inverse model causality. The piston velocity (v) is assumed to be positive during the extension movement of the piston while the piston force (F) is positive when the piston pulls the connected kinematics element. The following assumptions were done for the modelling: no internal leakages are considered, friction forces are neglected and the cavitation of the fluid is not considered.

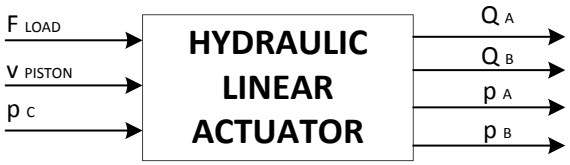

Fig. 3. Hydraulic Linear Actuator Inverse Model Causality.

According to the assumption done and to the defined conventions the flow rate at port A, Eq.(1), and at port B, Eq.(2), are calculated respectively as:

$$Q_A = A_A \cdot v \tag{1}$$

$$Q_B = -A_B \cdot v \tag{2}$$

The chambers pressures are defined knowing the piston velocity (v) sign, which discriminates the utilized equations. If the piston velocity is greater or equal to zero, the exploited equations are (3) and (4); otherwise (5) and (6):

$$p_B = p_C \tag{3}$$

$$p_A = \frac{F}{A_A} + p_B \cdot \frac{A_B}{A_A} \tag{4}$$

$$p_A = p_C \tag{5}$$

$$p_B = -\frac{F}{A_B} + p_A \cdot \frac{A_A}{A_B} \tag{6}$$

The counter pressure (p_C) is due to the resistance introduced by the outlet orifice of the valve section controlling the user.

2.2.2 Hydraulic Motor

Figure 4 shows the hydraulic motor inverse model causality. No internal and external leakages are considered, friction forces are neglected and the fluid cavitation is not considered.

Fig. 4. Hydraulic Motor Inverse Model Causality.

If the turret angular velocity (ω) is greater or equal to zero (i.e. a clockwise turret rotation is performed) the flow rates at ports A and B as well as the pressures A and B are defined through Eq.s (7) – (10):

$$Q_A = \frac{\omega_{TURRET} \cdot V_d}{\eta_v} \tag{7}$$

$$Q_B = -Q_A \tag{8}$$

$$p_B = p_C \tag{9}$$

$$p_A = p_B + \frac{T_{TURRET} \cdot 2\pi}{V_d \cdot \eta_{hm}} \tag{10}$$

If a counter clockwise turret rotation is performed, i.e. the turret angular velocity (ω) is lower than zero, the flow rates and the pressures at ports A and B are calculated with Eq.s (11) – (14):

$$Q_A = -Q_B \tag{11}$$

$$Q_B = -\frac{\omega_{TURRET} \cdot V_d}{\eta_v} \tag{12}$$

$$p_A = p_C \tag{13}$$

$$p_B = p_A + \frac{T_{TURRET} \cdot 2\pi}{V_d \cdot \eta_{hm}} \tag{14}$$

The volumetric and the hydraulic-mechanical efficiencies are considered as constants.

2.2.3 Valve Section

Figure 5 shows the valve section inverse model causality assumed for the input/output variables. If an extension movement of the linear actuator or a clockwise rotation for the turret is performed Q_A will be positive, otherwise for a retraction movement of the linear actuator or a counter clockwise rotation of the turret Q_A will be negative.

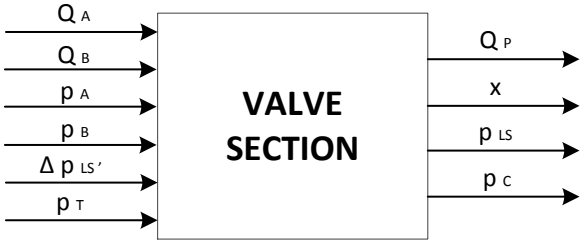

Fig. 5. Valve Section Inverse Model Causality.

If Q_A is greater or equal to zero the Eq.s (15) – (18) are exploited in order to evaluate the output variable from the valve section inverse model:

$$Q_P = Q_A \tag{15}$$

$$p_{LS} = p_A \tag{16}$$

$$A_{IN}(x) = A_A(x) = \frac{Q_P}{cd}\sqrt{\frac{\rho}{2 \cdot \Delta p_{LS}{}'}} \tag{17}$$

Form Eq.(17) the metering area is defined. The spool position (x) can be defined taking advantage of the correlation defined by the valve constructor. Always exploiting the valve constructor correlation the correspondent outlet area ($A_{OUT}(x) = A_B(x)$) can be defined.

$$p_C(x) = \frac{{Q_B}^2 \cdot \rho}{2 \cdot cd^2 \cdot A_{OUT}(x)^2} + p_T \tag{18}$$

If Q_A is lower than zero the Eq.s (19) – (22) are exploited in order to evaluate the output variable from the valve section inverse model:

$$Q_P = Q_B \tag{19}$$

$$p_{LS} = p_B \tag{20}$$

$$A_{IN}(x) = A_B(x) = \frac{Q_P}{cd}\sqrt{\frac{\rho}{2 \cdot \Delta p_{LS}{}'}} \tag{21}$$

Form Eq.(21) the metering area is defined. The spool position (x) can be defined taking advantage of the correlation defined by the valve constructor. Always exploiting the valve constructor correlation the correspondent outlet area ($A_{OUT}(x) = A_A(x)$) can be defined.

$$p_C(x) = \frac{{Q_A}^2 \cdot \rho}{2 \cdot cd^2 \cdot A_{OUT}(x)^2} + p_T \tag{22}$$

2.2.4 Pump and Regulators

Figure 6 shows the pump and its regulators inverse model causality assumed for the input/output variables.

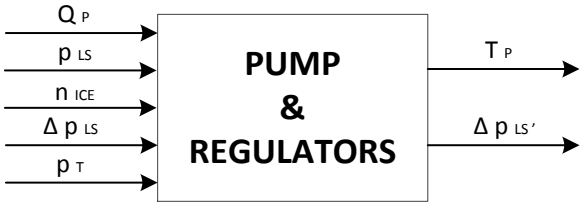

Fig. 6. Pump and Regulators Inverse Model Causality.

The required torque from the pump is defined taking advantage of a map based correlation defined with the aid of the pump direct causality mathematical model. The map inputs are the pump delivery flow rate (Q_P), the pump differential pressure (Δp_P) and the engine speed (n_{ICE}). The following Eq.s are utilized to define the required variables:

$$\Delta p_P = p_D - p_{Tank} \tag{23}$$

$$p_D = p_{LS} + \Delta p_{LS}{}' \tag{24}$$

Being the pump torque limited by its torque limiter, in order to avoid engine stall or shutdown, the instantaneous LS margin pressure ($\Delta p_{LS}{}'$) is defined according Eq.s (25) or (26):

$$\Delta p_{LS}{}' = \Delta p_{LS} \qquad if\ \ T_P < T_{ICE_{MAX}}(n) \tag{25}$$

$$\Delta p_{LS}{}' = \Delta p_{LS} - \Delta p_{LIM}(Q_P, p_{LS}, T_P) \qquad if\ \ T_P \geq T_{ICE_{MAX}}(n) \tag{26}$$

2.2.5 Engine

Figure 7 shows the engine inverse model causality assumed for the input/output variables. The fuel mass flow rate (*mf*) is defined taking advantage of a map based correlation defined with the aid of the engine direct causality mathematical model. The map inputs are the engine speed (n_{ICE}) set to be constant and the pump required torque (T_P).

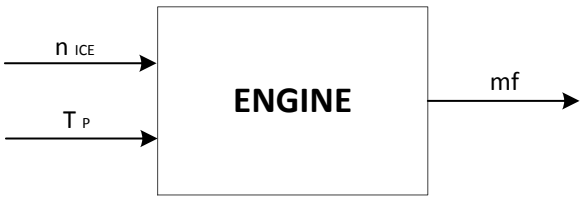

Fig. 7. Engine Inverse Model Causality.

2.2.6 Hydraulic Accumulator

A bladder type hydraulic accumulator has been considered in order to allow energy recovery during braking and load lowering phases in the working cycle. The accumulator (pre-charged with gaseous Nitrogen) is modeled assuming an adiabatic compression following a polytropic gas law (27):

$$p \cdot V^{\gamma} = const \tag{27}$$

Differentiating Eq. (27), pressure changes in the accumulator are obtained from the differential Eq. (28):

$$\frac{dp}{dt} = -\gamma \cdot \frac{p}{V} \cdot \frac{dV}{dt} \tag{28}$$

The volume variations depend on the inlet and outlet oil flow rate.

2.2.7 Complete excavator inverse causality model

Figure 8 depicts the complete model of the basic excavator layout (Figure 1) in the inverse causality representation. This model has been implemented in the Simulink® environment and will be used to perform the optimizations presented in the following sections.

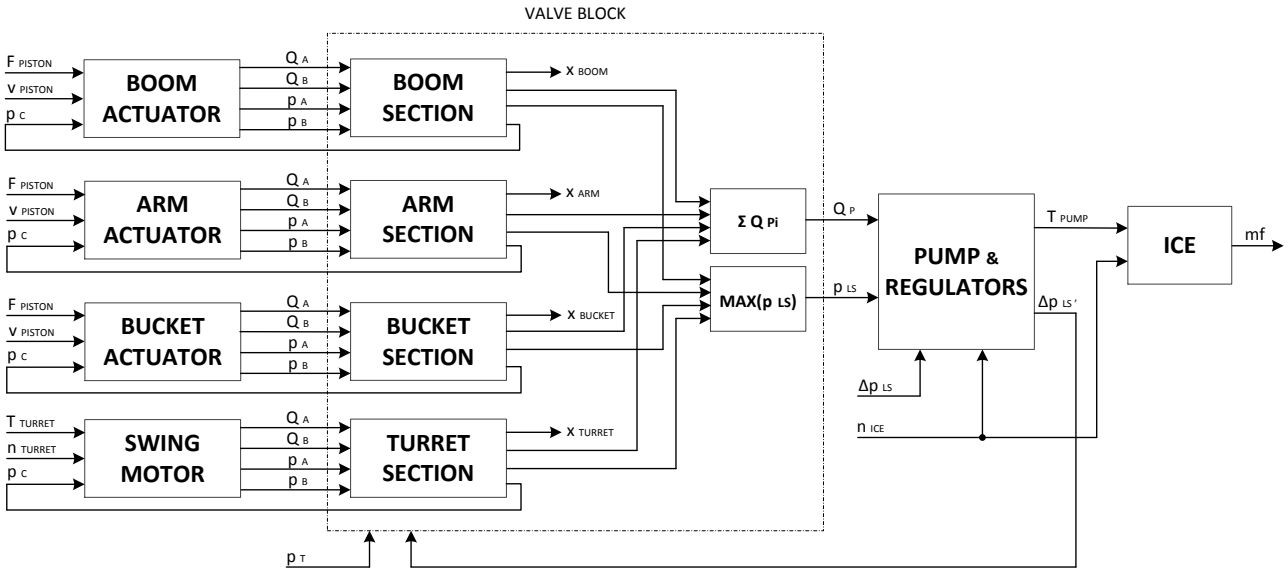

Fig.8. Inverse Causality Model of the Standard Excavator.

2.3 Reference Working Cycle

Fuel consumption is strictly related to the machinery overall efficiency and is actually one of the main performance parameter used when comparing different machinery. Since fuel consumption strongly depends on the operating conditions as well as on the machinery layout and management strategy, the definition of a proper "benchmark" in terms of a significant working cycle is crucial. Many different working cycles have been defined, some commercial and others standardized. The Japan Construction Mechanization Association (JCMAS) has defined a standardized earth-moving machinery test procedure to evaluate the fuel consumption on hydraulic excavators, the JCMAS H20:2007 [*16*]. This standardized working cycle does not involve any bucket-soil interaction, in order to not introduce stochastic effect on the measuring, and it is composed of four different operating modes: digging and loading motion; leveling motion; travelling motion and idling functioning. For each of them the JCMAS standard defines the sequential movements and the kinematics elements positioning, the engine rotational speed and the timing. Once fuel consumption has been calculated for each operating mode, the overall fuel consumption during a typical working hour can be estimated according with the procedure defined by the standard. The direct causality model of the standard excavator was exploited to performing the simulations of the previously mentioned standardized working cycles, defining the references (i.e. standard machine fuel consumption) for the comparisons.

Starting from the trajectories prescribed by the standard and knowing masses and geometries of the excavator components, the velocities of the hydraulic actuators and, from dynamic equilibrium, the exerted forces to the actuators can be obtained from the direct excavator model. This forces and velocities are also used for the simulations of the reverse causality model.

Figures 9 – 12 show the boom, arm, bucket and turret inputs relative to the digging and loading motion of the actuated user during the cycle.

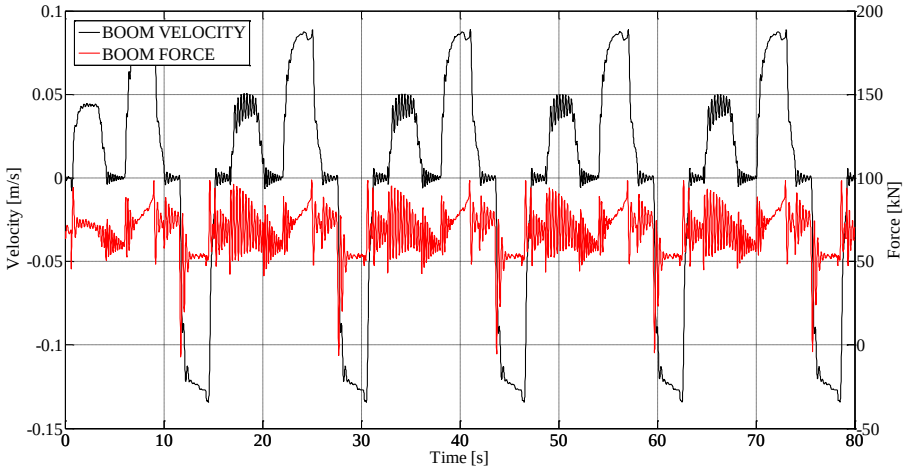

Fig.9. Boom Inputs – Digging and Loading motions.

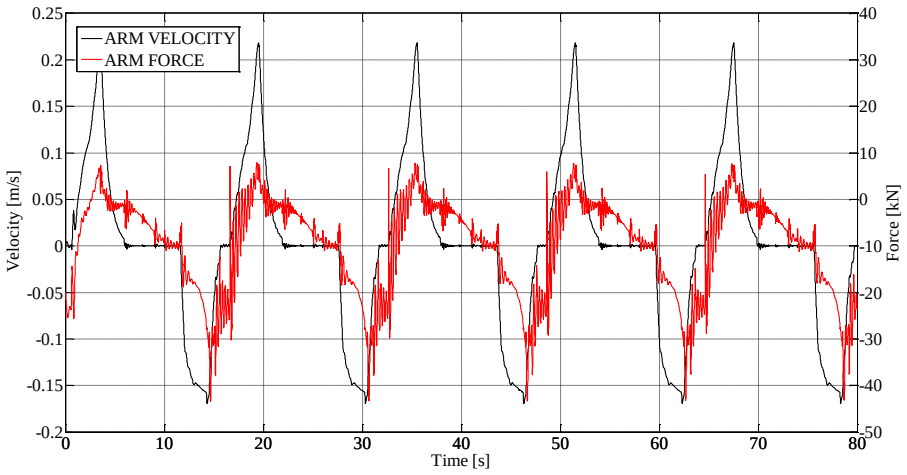

Fig.10. Arm Inputs – Digging and Loading motions.

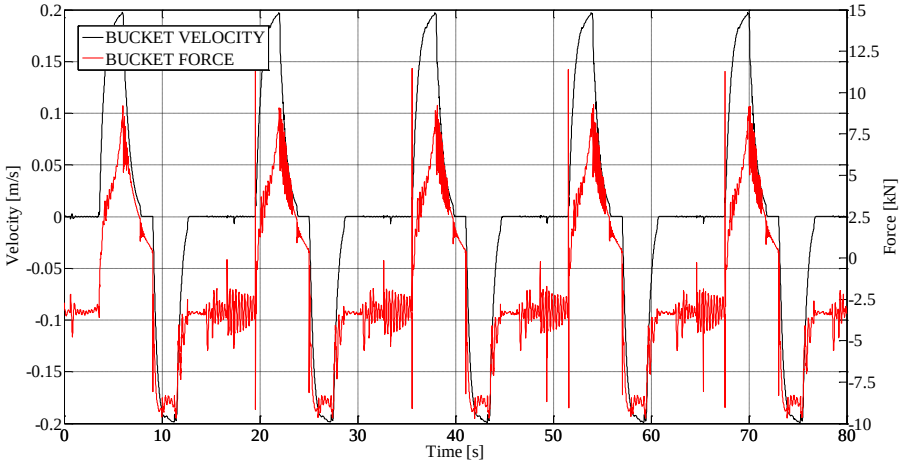

Fig.11. Bucket Inputs – Digging and Loading motions.

239

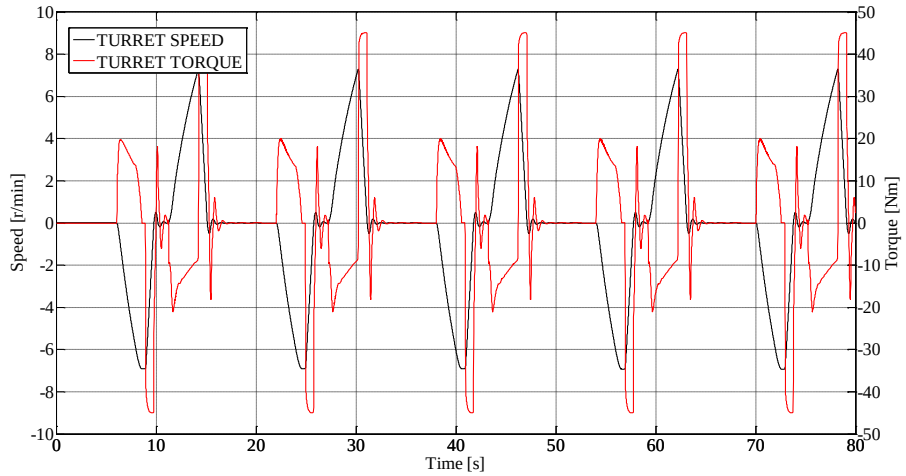

Fig.12. Turret Inputs – Digging and Loading motions.

240

241 Figures 13, 14 report the boom and arm defined inputs throughout the leveling motion respectively. During this

242 operating mode the bucket and the swing are not actuated.

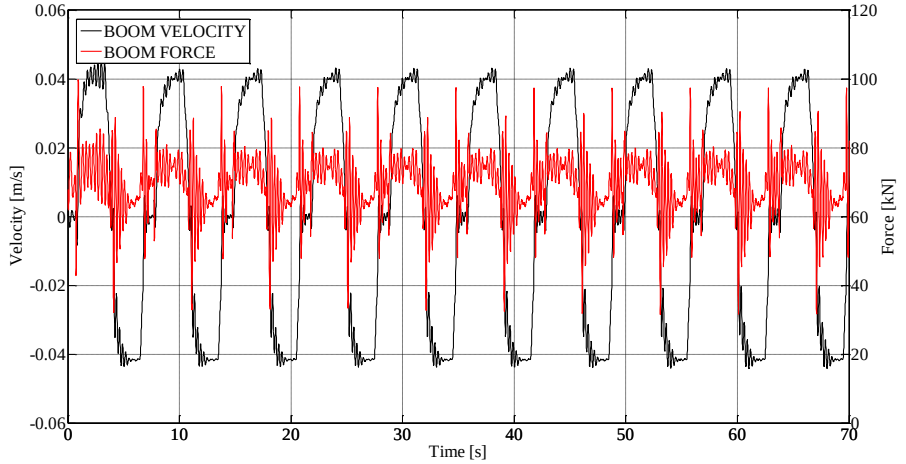

Fig.13. Boom Inputs – Leveling motion.

243

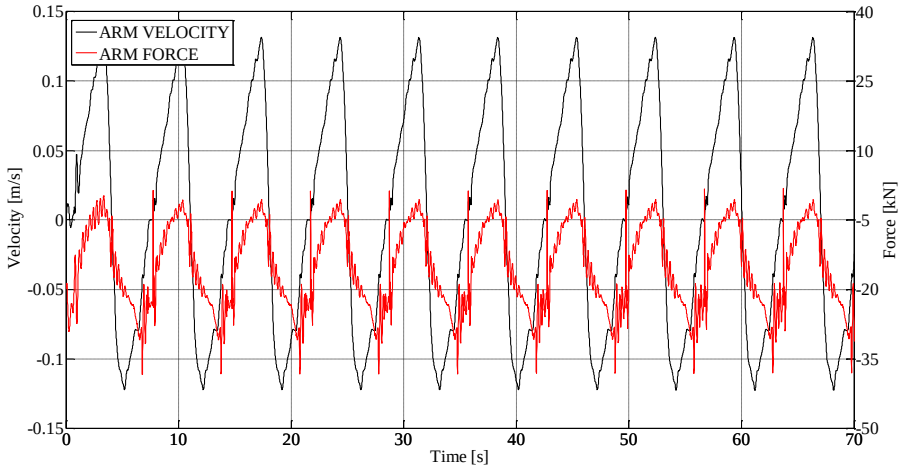

Fig.14. Arm Inputs – Leveling motion.

The travelling motion and the idling functioning were only performed with the direct causality model of the standard excavator because during these operating modes the energy recovery and reuse system will be never activated. Thus no differences between the proposed hybrid layouts will be pointed out.

2.4 Inverse Model Validation

To perform a comprehensive comparison between the proposed hybrid layouts and the reference one (the standard machinery layout), a validation of the inverse causality model of the standard excavator has to be performed firstly. The two models have been compared with reference to the previously described typical machinery working cycle. Starting from the illustrated profiles of forces and velocities of the various actuators, the remaining variables are calculated by means of the inverse causality model described in section 2.2.

Figures 15 – 18 report the comparison between the direct and the inverse causality models output variables during the simulations of the digging and loading motion of the JCMAS cycle.

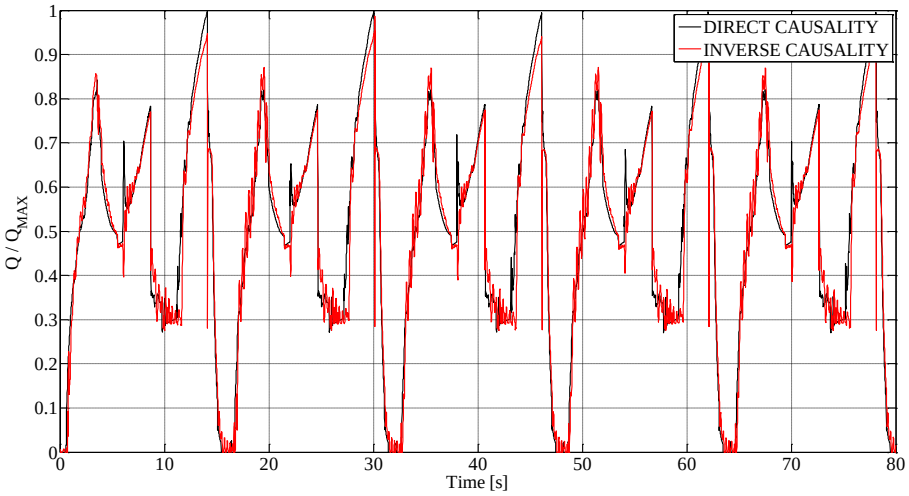

Fig.15. Comparison of pump outlet flow rate estimated from direct and inverse causality models.

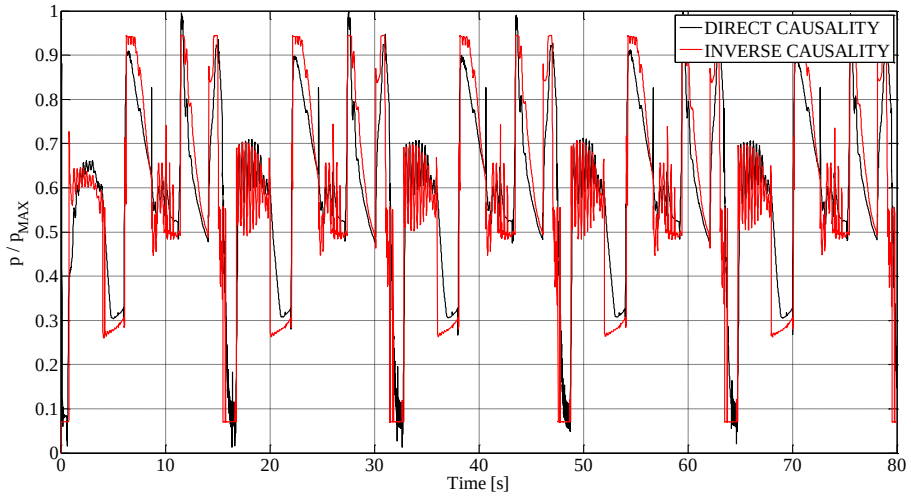

Fig.16. Comparison of pump delivery pressure estimated from direct and inverse causality models.

257

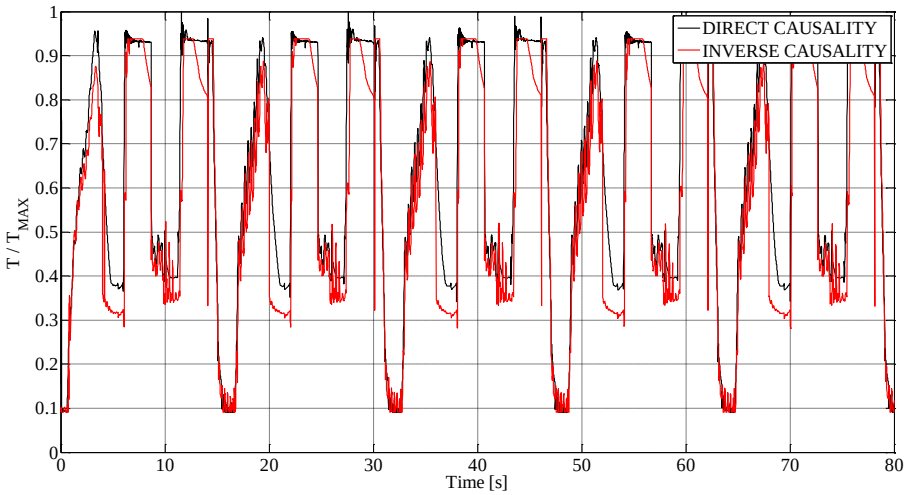

Fig.17. Comparison of engine torque estimated from direct and inverse causality models.

258

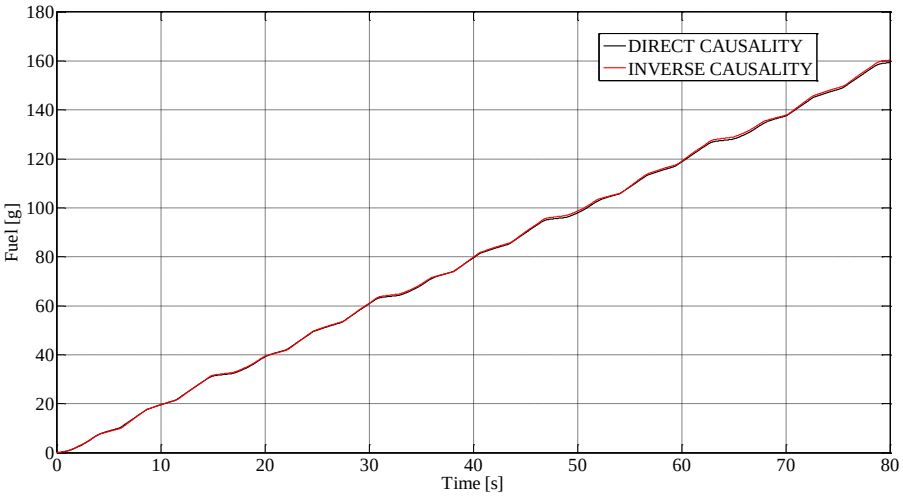

Fig.18. Comparison of fuel consumption estimated from direct and inverse models.

259

260 It is noticeable that, despite of the quasi-steady assumption, there is a great agreement between inverse and direct
261 causality models, with differences in the evaluation of fuel consumption lower than 1%.

3. Optimization problem definition

In order to apply the DP methodology to the fuel consumption minimization problem, system equations are rearranged in a discrete state space representation form, Eq.(29). Actuators solicitations are treated as known external disturbances, thus obtaining time invariant correlations *f* and *g*.

$$\begin{cases} x(k+1) = f(x(k), u(k), w(k)) \\ y(k) = g(x(k), u(k), w(k)) \end{cases} \tag{29}$$

For the examined problem, the state variable *x(k)* corresponds to the accumulator pressure *p* and the state update equation [*f(x(k),u(k),w(k))*] is derived from Eq. (28) with the term $\frac{dV}{dt}$ accounting for the net inlet flow rate, function of external disturbances and control valves actuation. The term *u(k)* is a vector representing the behavior of the set of controls valves regulating the flow to and from the accumulator, in the proposed hybrid layout under investigation. Its dimension is correlated to the specific adopted layout. Finally, *w(k)* represents the external disturbances acting on the actuators. Its components are listed in Eq.(30).

$$[F_{BOOM}(k), v_{BOOM}(k), F_{ARM}(k), v_{ARM}(k), F_{BUCKET}(k), v_{BUCKET}(k), T_{TURRET}(k), \omega_{TURRET}(k)] \tag{30}$$

where *F*, *v* (*T*, *ω*) represent the force and velocity (torque and rotational speed) on the generic actuator, derived in the previous section, and whose profile is determined from the simulated working cycles with the aid of the direct causality mathematical model of the standard machinery.

The output *y(k)* is the fuel mass flow rate burned by the ICE at every time step in order to guarantee the required power output. The time step Δt has been set to 0.01 *s*, which has been found to guarantee low computational time for problem resolution and good accuracy in the integration of the state space equation.

Some boundary constraints are added on accumulator pressure (to maintain safe operating conditions) and ICE engine torque (the torque request must be feasible):

$$x(k) \in \lfloor x_{min}, x_{max} \rfloor \tag{31}$$

$$T_{ICE}(k) \in \lfloor T_{ICE,min}(n_{ICE}), T_{ICE,max}(n_{ICE}) \rfloor \tag{32}$$

where $x_{min} \in [p_{MIN\,1}, \dots, p_{MIN\,i}, \dots, p_{MIN\,N}]$bar (depending on the accumulator design), $x_{max} = 4 \cdot x_{min}$ and minimum/maximum engine torques $T_{ICE,min/max}$ are correlated to the instantaneous ICE speed (n_{ICE}).

The objective of the optimization is the minimization of the *J* cost corresponding to the fuel consumption during the working cycle:

$$J_\pi(x_0) = \sum_{k=1}^{N-1} y(k) \cdot \Delta t \tag{33}$$

Where $x_0 = x(p_{MIN\,i})$ is the initial accumulator pressure, chosen equal to x_{min} , and $\pi = \{\overrightarrow{u_0},\ \overrightarrow{u_1}, \dots, \overrightarrow{u_N}\}$ is the generic control policy adopted on the valve controlling the energy storage. No additional terms are introduced regarding accumulator final state $x_f = x(N)$.

For the various proposed layouts and for the every combination of the bladder accumulator parameters (volume, initial pressure), the objective of the optimization is the determination of the optimal control policy π^* minimizing fuel consumption:

$$\pi^* = \arg\ min_\pi\ J_\pi(x_0) \tag{34}$$

The corresponding cost $J^* = J_{\pi^*}(x_0)$ would be used in the comparison of different system layouts and pressure accumulator sizing.

3.1 DP algorithm

The evaluation of the optimal control policy is carried out by means of a DP algorithm which exploits Bellman principle of optimality [*13*] stating that an optimal policy has the property that whatever the initial state and initial decision are, the remaining decisions must constitute an optimal policy with regard to the state resulting from the first decision, which is equal to say that, given an optimal control policy $\pi^* = \{\overrightarrow{u_0}, \dots \overrightarrow{u_\iota}, \dots, \overrightarrow{u_N}\}$, for the optimization problem $min_\pi\ J_\pi(x_0)$, the truncated policy $\pi^*{}_K = \{\overrightarrow{u_k}, \overrightarrow{u_{k+1}}, \dots, \overrightarrow{u_{k+\iota}}, \dots, \overrightarrow{u_N}\}$ with $k > 1$ is still optimal for the "tail sub-problem" $min_\pi\ J_\pi(x_k)$. Thus, the principle of optimality suggests that an optimal policy can be constructed in piecemeal fashion, first constructing an optimal policy for the "tail sub-problem" involving the last stage, then extending the optimal policy to the "tail sub-problem" involving the last two stages, and continuing in this manner backward until an optimal policy for the entire problem is constructed.

The implementation of the DP algorithm to the excavator model is done by means of a Matlab® function developed by [*23*].

4. Hydraulic Hybrid Excavator Layouts

4.1 Proposed Hybrid Layouts

In this section the investigated hydraulic hybrid layouts of the excavator under study are presented. Although many different combinations of solution could be in general proposed and investigated for excavators, in this paper only

energy recovery from boom and turret have been considered. The proposed layouts features are reported in Tab.1. The actuators involved in energy recovery and the numbers of energy storage devices (bladder accumulators) are stated for each case.

Tab.1. Considered Layouts for the Hybrid System.

CIRCUIT LAYOUT	ACTUATOR(S)	NUMBER OF ACCUMULATOR(S)
A	Boom	1
B	Turret	1
C	Boom - Turret	1
D	Boom - Turret	2

The ISO schemes of the proposed layouts of Tab.1 are shown in Figs. 19 – 22. The travel motors and the relative flow control valve sections have not been reported for simplicity because the layouts do not involve those users for energy recovery. A common component for each of the layouts is a fixed displacement external gear hydraulic motor, installed to reuse the energy stored during the accumulation phases. The hybrid configurations exploiting boom lowering are also equipped with a variable flow control orifice (VCO), placed between the hydraulic actuator and the accumulator, which prevents cavitation into the actuator rod side and maintains control on the user velocity during the energy recovery phase. The VCO spool displacement is proportional and synchronized with the main spool displacement of the boom valve section. The proposed optimization methodology, based on the DP algorithm, has been exploited to define the optimal control laws for the introduced components (i.e. recovery and reuse valves) in the presented hybrid layouts. The recovery and reuse valves opening are assumed to be ON/OFF. Considering the solution A, Fig.19, the control laws (u_1, u_2) govern the opening of the corresponding valves, enabling or avoiding energy storage and/or recovery. For solution B, Fig.20, concerning the swing deceleration phases, the DP algorithm has been only used to define the recovery control law (u_1) which enables the energy reuse only, since the energy recovery phases are directly dependent by the user main valve spool positioning ($f(x_{TURRET})$). Solutions C and D, Figs. 21 – 22, are a combination of the solutions A and B, and for each of them the DP algorithm has been used to define (u_1), (u_2) and (u_1), (u_2), (u_3), (u_4) respectively.

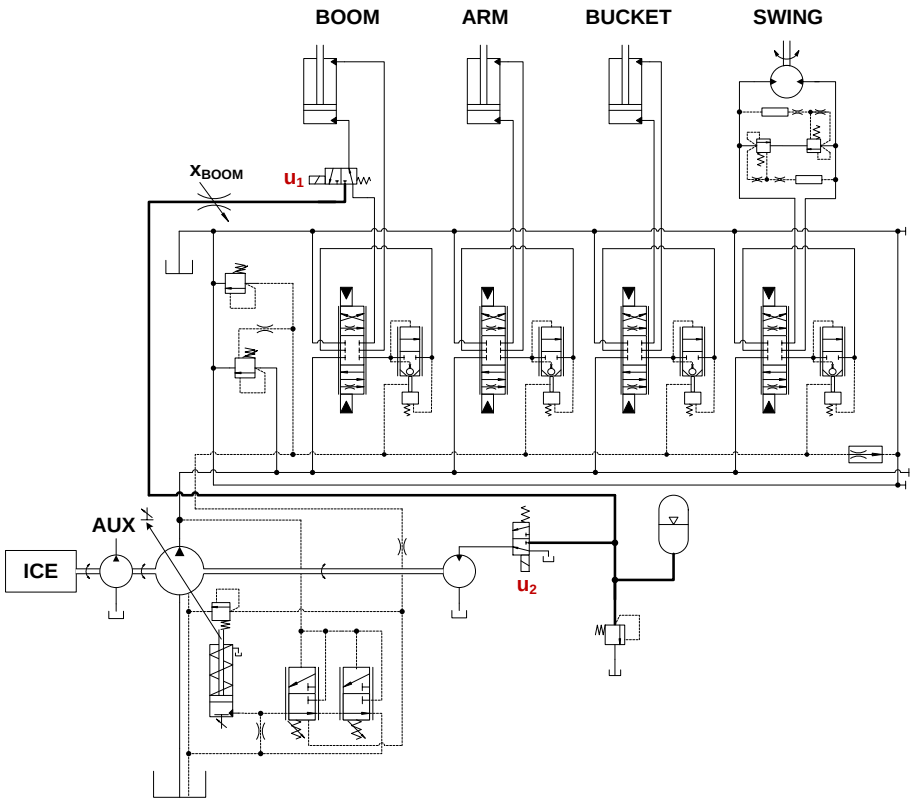

335

336 **Fig.19**. ISO Scheme of the Hybrid Layout A.

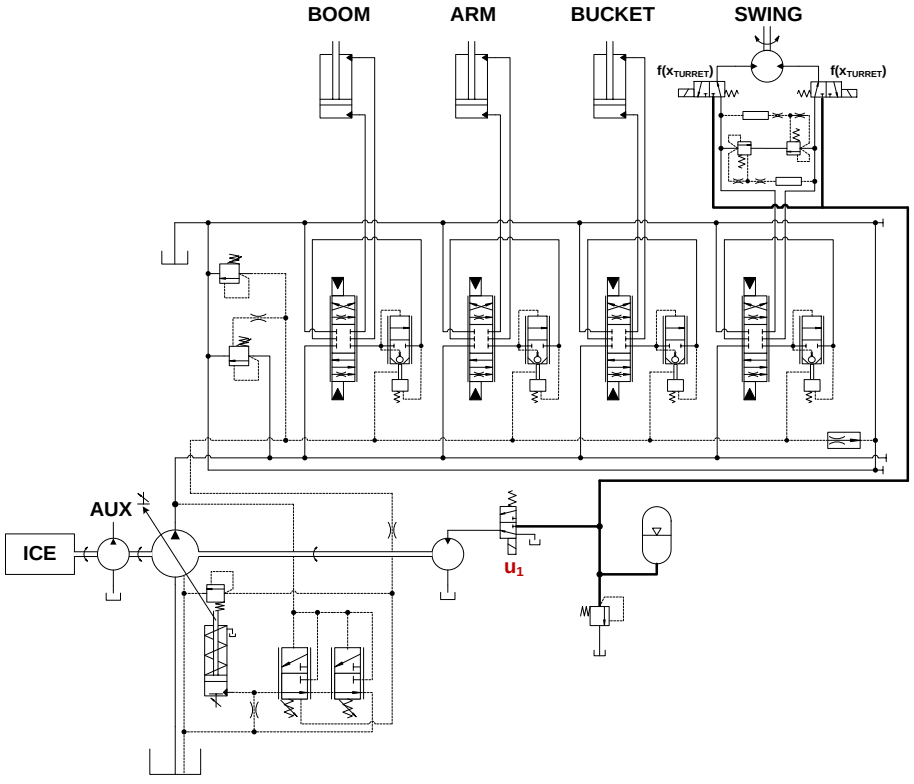

337

338 **Fig.20**. ISO Scheme of the Hybrid Layout B.

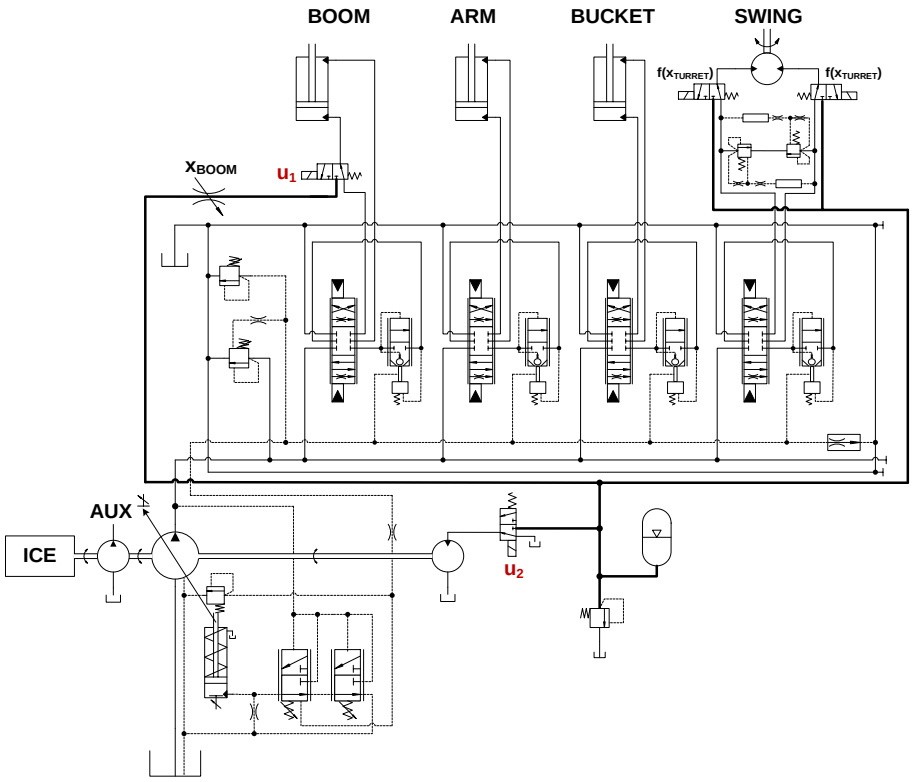

339

340 **Fig.21**. ISO Scheme of the Hybrid Layout C.

341

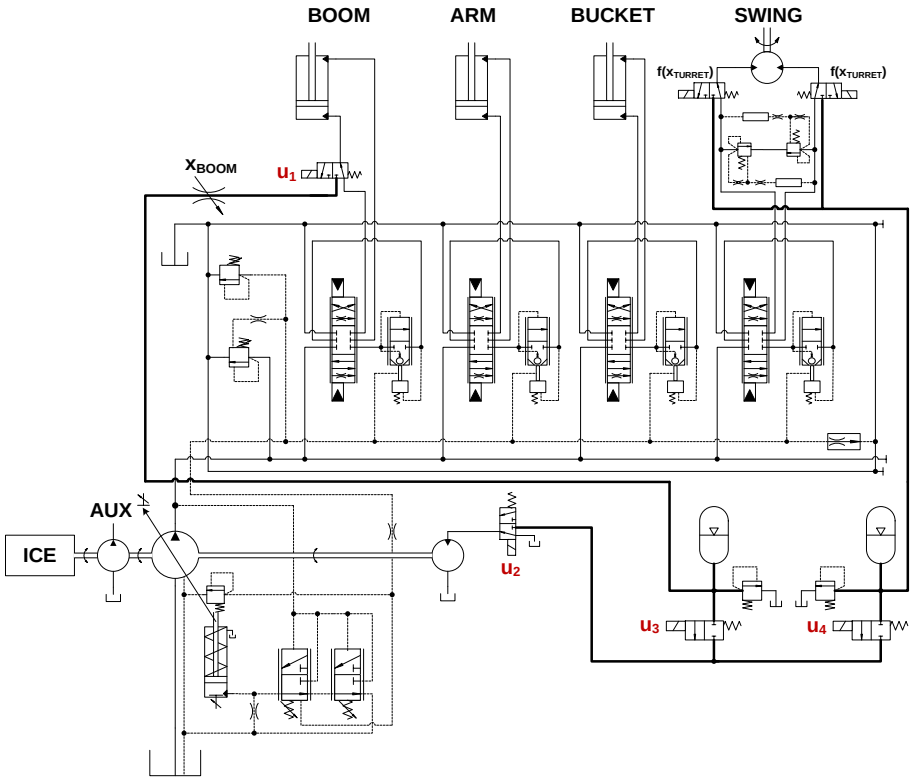

342

343 **Fig.22**. ISO Scheme of the Hybrid Layout D.

344

On the basis of the inverse causality model of the standard excavator, the inverse causality models of the proposed hybrid layouts under investigation were defined. As examples Figs. 23 – 24 depict the inverse causality models of the hybrid layouts A and B; layouts C and D are a combination of these.

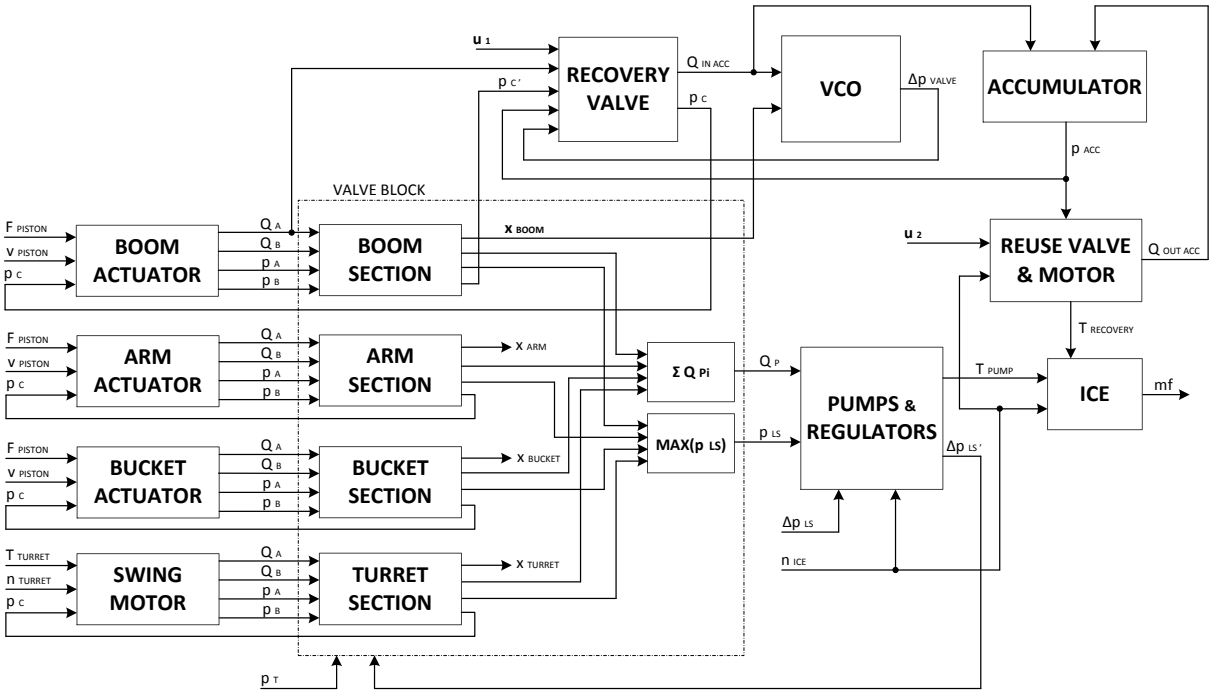

Fig.23. Inverse Causality Scheme of the Hybrid Layout A.

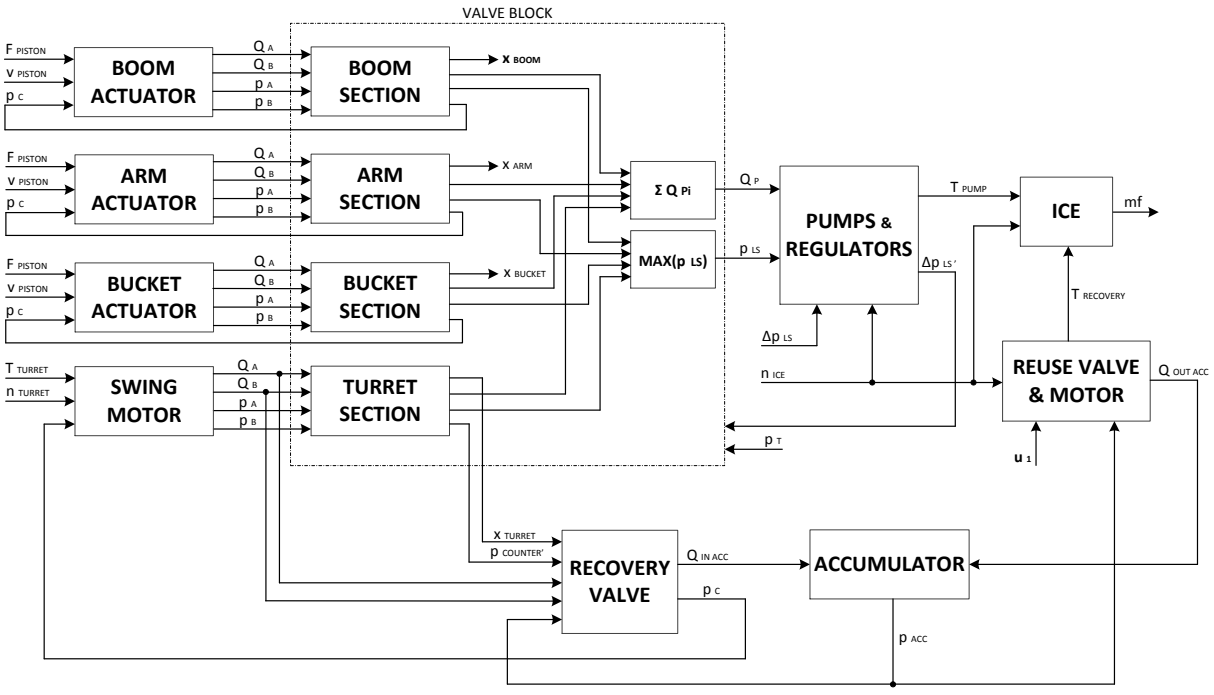

Fig.24. Inverse Causality Scheme of the Hybrid Layout B.

4.2 Hybrid Layouts Optimal Sizing

To perform a comprehensive comparison in order to define the solution which enables the best fuel saving performance, the different proposed hybrid layouts have to be compared in their optimal configuration. This means that the components introduced into the hybrid layouts have to be optimally sized.

The optimization target is that of minimize the fuel consumption during the performed working cycle. As for an excavator the digging and loading movement are the most important phases during the typical working hour defined in [*16*], this sub-cycle has been selected for the components optimization procedure.

The parameters of interest for the optimal dimensioning procedure are the accumulator minimum working pressure (p_{MIN}) and the accumulator volume (V_0) for all the proposed hybrid layouts. When the energy recovery from the boom is also an option, the equivalent diameter (d_{EQ}) of the VCO is an additional parameter to be optimally sized.

The dimensioning procedure has been done through a DoE (Design of Experiment) methodology, where a discrete grid of possible values for the parameters of interest has been defined in order to explore the different parameter combination still maintaining a reliable functioning of the system and the components. The variation ranges of the parameters involved in the optimization are: $p_{MIN} \in [10;\ 50]$ bar with an increasing step of 5 bar for the layout A and $p_{MIN} \in [10;\ 100]$ bar with an increasing step of 10 bar for the layout B; $V_0 \in [2.5, 4, 5, 6, 10]$ L according with the available accumulators; $d_{EQ} \in [1;\ 8]$ mm with an increasing step of 0.5 mm (only for layout A, C, D). For each hybrid layout and for each possible parameter combination the DP algorithm defines the optimal control strategy for governing the recovery and reuse valves.

5. Hybrid Layout Comparison

This section present the results of the optimization performed with the aim of define the optimal combination of the accumulator minimum pressure, accumulator volume and the equivalent diameter of the VCO of the boom (only for the layouts that involve the energy recovery from it) as previously stated. The optimization has been performed for the digging and loading motion defined in [*16*]. Sections 5.1 and 5.2 report the results concerning layouts A and B respectively, while results about layouts C and D have not been reported for brevity. Finally once defined the optimal sizing of the components of interest the complete JCMAS working cycle has been performed for all the proposed layouts. The final results are reported in section 5.3 where a quantitative comparison based on fuel consumption is presented. The fuel saving percentages are referred to the standard layout fuel consumption.

383 **5.1 DP Results: Layout A**

384 Figures 25 – 29 report some of the results obtained through the DoE methodology presented in section 4.2 and applied
385 to the layout A. Being the energy recovery from the boom considered in this configuration, the sizing procedure
386 involves the accumulator minimum pressure (p_{MIN}), the accumulator volume (V_0) and the equivalent diameter of the
387 VCO (d_{EQ}). The reported charts represent the fuel saving percentage, referring to the standard layout, during the
388 digging and loading motion defined in [16] at different accumulator minimum pressure levels.

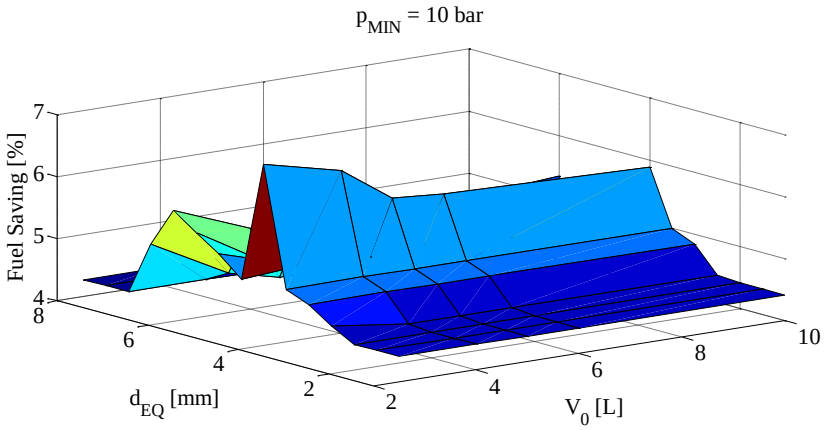

389

390 **Fig. 25**. Layout A Fuel Saving Percentage [$p_{MIN} = 10\ bar$].

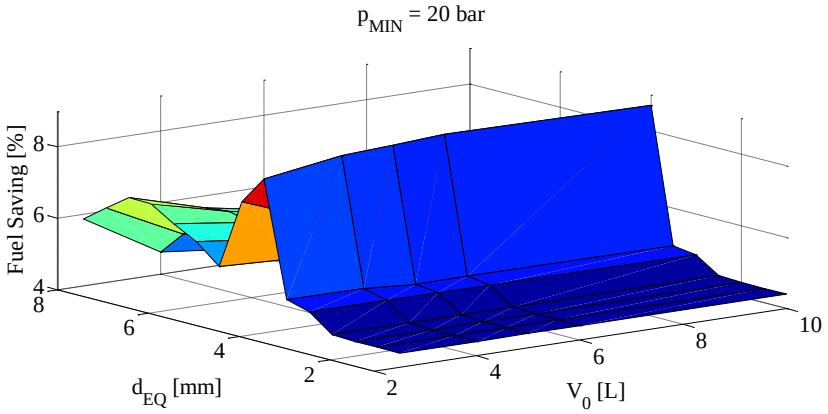

391

392 **Fig. 26**. Layout A Fuel Saving Percentage [$p_{MIN} = 20\ bar$].

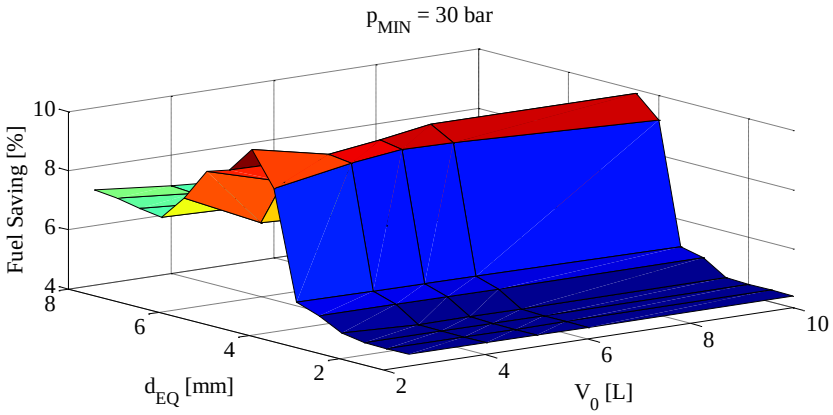

393

394 **Fig. 27**. Layout A Fuel Saving Percentage [$p_{MIN} = 30\ bar$].

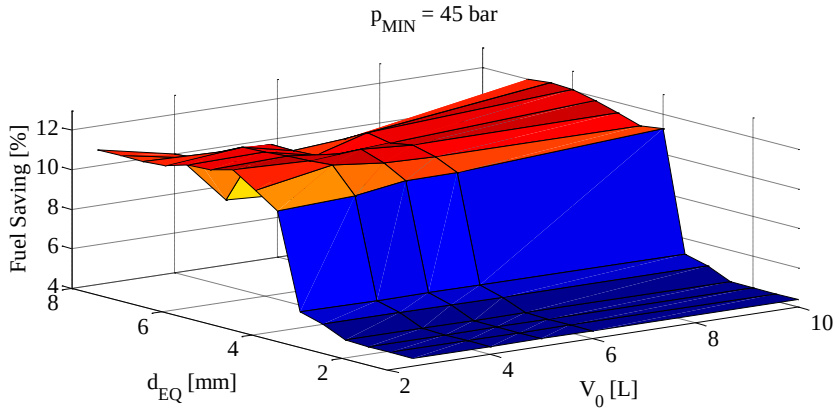

395

396 **Fig. 28**. Layout A Fuel Saving Percentage [$p_{MIN} = 45\ bar$].

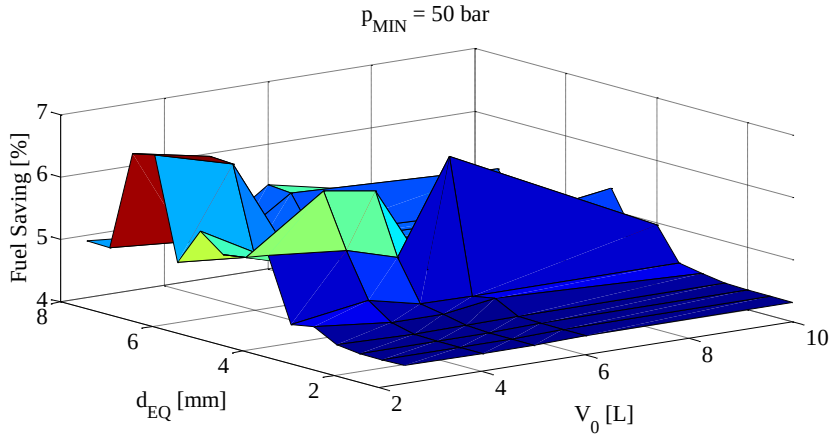

397

398 **Fig. 29**. Layout A Fuel Saving Percentage [$p_{MIN} = 50\ bar$].

399

400 As can be observed from the Figs. 25 – 29, for each combination of the considered parameters is possible to define a
401 maximum percentage of fuel saving. Comparing the overall results obtained for the layout A, the best parameters
402 combination which achieves the overall maximum fuel saving percentage could be identified: minimum accumulator
403 working pressure $p_{MIN} = 45\ bar$, accumulator volume $V_0 = 10\ L$; VCO equivalent diameter $d_{EQ} = 6.5\ mm$. This
404 parameter setting define the layout A best configuration while the DP optimal control laws (u_1, u_2) are applied
405 governing the opening of the corresponding valves of Fig. 19 defining the instantaneous accumulator pressure. Figure
406 30 reports the layout A optimal control laws and the correspondent accumulator pressure during a complete digging
407 cycle (five sequential repetitions), while Fig.31 shows an intermediate digging cycle for a better understanding of the
408 optimal control laws.

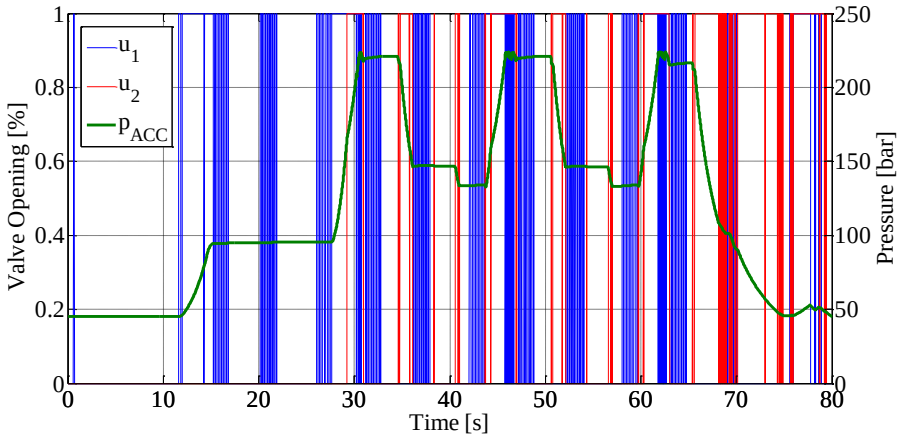

Fig. 30. Valves Optimal Control Policy (u_1, u_2) - Layout A

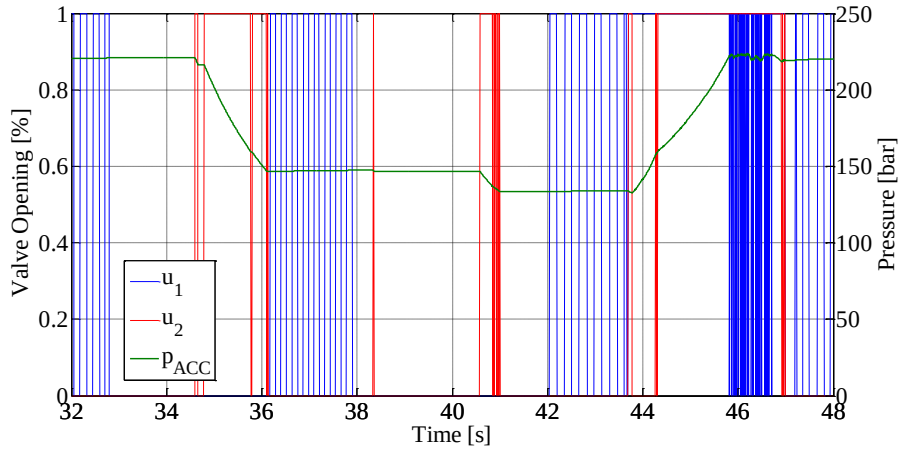

Fig. 31. Accumulator Pressure (p_{ACC}) of the Optimal Layout A Configuration.

5.2 DP Results: Layout B

Figure 32 report the DoE results for the hybrid layout B, presented in section 4.1, where only the energy recovery from the turret braking is considered. The sizing procedure only involves the accumulator minimum working pressure (p_{MIN}) and the accumulator volume (V_0). The reported chart represents the fuel saving percentage, referring to the standard layout, during the digging and loading motion defined in [16]. The optimal combination of the accumulator parameters which maximize the fuel saving percentage are: minimum accumulator working pressure $p_{MIN} = 100\ bar$, accumulator volume $V_0 = 2.5\ L$.

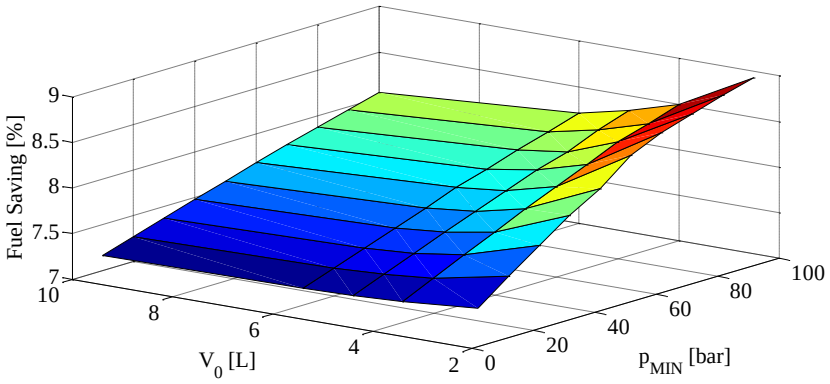

Fig. 32. Layout B Fuel Saving Percentage Chart.

Figure 33 reports the optimal control law, associated to the optimal accumulator sizing parameter, governing the reuse valve opening (u_1) and the correspondent accumulator pressure (p_{ACC}), referring to Fig. 24 layout, during the digging and loading cycle performed.

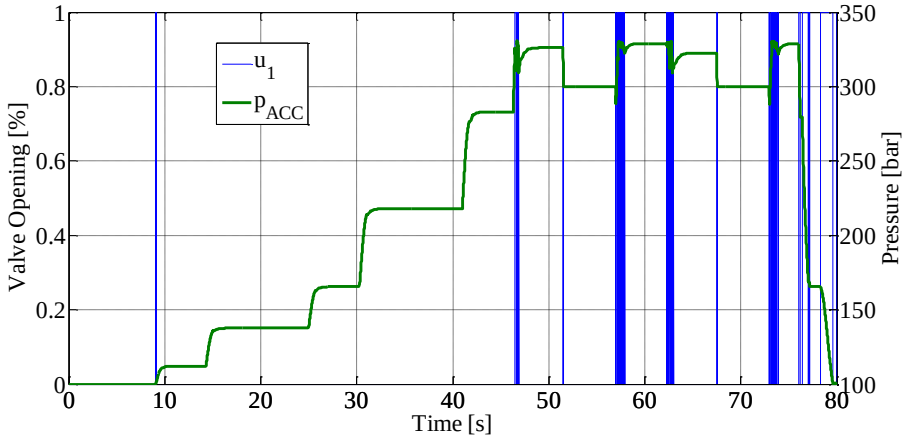

Fig. 33. Valve Optimal Control Policy (u_1) and Accumulator Pressure (p_{ACC}) - Layout B

5.3 Layout Comparison

Once defined the optimal sizing parameters for the accumulator and for the VCO (where required), for each proposed hybrid layout, it is possible to evaluate the fuel consumption over the complete working cycle defined in [*16*], with reference to the baseline configuration (i.e., the original configuration), thus obtaining the percentage reduction in fuel consumption per working hour. This final procedure makes possible to compare in a comprehensive manner the proposed hybrid layout in their optimal configuration. Table 2 summarizes the overall fuel saving percentages.

Tab.2. Percentage of fuel savings from the baseline for the considered Hybrid Circuit Layouts.

CIRCUIT LAYOUT	ACTUATOR(S)	NUMBER OF ACCUMULATOR(S)	FUEL SAVED
A	Boom	1	10 – 11 %
B	Turret	1	2 – 3 %
C	Boom - Turret	1	11 – 12 %
D	Boom - Turret	2	13 – 14 %

436 Optimizations A and B yields an optimal accumulator size of respectively 10 L (energy recovery from boom lowering),
437 and 2.5 L (energy recovery from turret swing). As the two values are very different, when using a single common
438 accumulator for the two energy recovery tasks (layout C) the sizing of the accumulator is somehow a compromise
439 between the two and the resulting fuel consumption reduction is lower than what can be achieved in design D where the
440 two accumulators allow for a better exploitation of the available energy.
441

442 ## 6. Conclusion

443 A hybridization comparison methodology based on DP algorithm has been presented in detail in this paper. The
444 methodology require some essential steps in order to be exploited: 1, the definition and the validation of the inverse
445 causality mathematical model for the considered system; 2, the definition of a reference working cycle, 3, the definition
446 of the different hybrid layout to be investigated and compared; 4, the definition of the solution of the control
447 optimization problem through a DP algorithm (for each proposed layout); 5, a DoE based optimization of the additional
448 components sizing.
449 The presented methodology defines for each proposed hybrid layout both the optimal components size and the optimal
450 control strategy. The optimal control strategy defined represents only a benchmark for a further definition of online
451 control strategies.
452 This hybridization comparison methodology has been successfully applied to a middle size hydraulic excavator as a
453 baseline example. The machinery hydraulic system mathematical model has been realized and validated in both direct
454 and inverse causality. Several different hybrid layouts of the excavator under study have been proposed and compared
455 by means of the presented hybridization methodology.
456 On the basis of the obtained results on the JCMAS working cycle for this machine size, it is understood that energy
457 recovery from the boom is far more effective then energy recovery from the turret.
458 Finally, this approach permits to obtain the best components sizing combination for the hybrid layouts considered, an
459 optimal control policy for each layout, and allows to choose the hybrid layout configuration able to yield the highest
460 fuel saving percentage with reference to the standard configuration.
461 Future works, based on the presented methodology, will concern the development of algorithms for the definition and
462 the implementation of online control strategy starting from the defined optimal control strategy of the selected hybrid
463 layout.
464

References

1. J. Zimmermann, M. Ivantysynova.. Reduction of Engine and Cooling Power by displacement Control. Proc. of 6th FPNI-PhD Symp. (2010) West Lafayette, USA.
2. M. Inderelst, S. Losse, S. Sgro, H. Murrenhoff. Energy efficient system layout for work hydraulic of excavators. 2011. The twelfth Scandinavian International Conference on Fluid Power.
3. A. Gambarotta, P. Casoli, N. Pompini, L. Riccò (2014) .Co-simulation and control-orientated modeling in the development of a hydraulic hybrid system" , 14th Stuttgart International Symposium "Automotive and Engine Technology" Stoccarda (D) 18-19 Marzo 2014.
4. P. Casoli, A. Gambarotta N. Pompini, L. Riccò (2015) "Coupling excavator hydraulic system and internal combustion engine models for the Real-Time simulation" Control Engineering Practice (2015), pp. 26-37 DOI information: 10.1016/j.conengprac.2015.04.003.
5. R. Finzel, S.Helduser. Energy-Efficient Electro-Hydraulic Control Systems for Mobile Machinery/ Flow Matching, 6th IFK, Dresden, Germany, 2008.
6. Y.L. Cho, D.S. Jang, K.Y. Kim. Development of Energy Efficient Electro-Hydraulic System for Excavator. 7th IFK, Aachen 2010.
7. C. Musardo, G. Rizzoni, Y. Guezennec , B. Staccia. A_ECMS: An adaptive algorithm for hybrid electric vehicle energy management. European Journal of Control (2005) 11: 509-524.
8. Q. Xiao, Q. Wang, Y. Zhang. Control strategy of power system in hybrid hydraulic excavator. Automation in construction 17 (2008) 361-367. doi: 10.1016/j.autcon.2007.05.014.
9. D. Wang, C. Guan, S. Pan, M. Zhang, X. Lin. Performance analysis of hydraulic excavator powertrain hybridization. Automation in construction 18 (2009) 249-257. doi: 10.1016/j.autcon.2008.10.001.
10. T. Lin, Q. Wang, B. Hu, W. Gong. Research on the energy regeneration systems for hybrid hydraulic excavators. Automation in construction 19 (2010)1016-1026. doi: 10.1016/j.autcon.2010.08.002.
11. T. Wang, Q. Wang, T. Lin. Improvement of boom control performance for hybrid hydraulic excavator with potential energy recovery. Automation in construction 30 (2013) 161-169. http://dx.doi.org/10.1016/j.autcon.2012.11.034.
12. M. Erkkila, F. Bauer, D. Feld. Universal energy storage and recovery system – A novel approach for hydraulic hybrid. The 13th Scandinavian International Conference on Fluid Power, SICFP2013, June 3-5, 2013, Linkoping, Sweden. ISBN 978-91-7519-572-8.
13. R.E. Bellman. 1957. Dynamic Programming. Princeton University Press, NJ, USA.
14. B.C. Chen, Y.Y. Wu, H.C. Tsai. Design and analysis of power management strategy for range extend electric vehicle using dynamic programming. Applied energy 113(2014)1764-1774. http://dx.doi.org/10.1016/j.apenergy.2013.08.018.
15. M. Sprengel and M. Ivantysynova. Investigation and Energetic Analysis of a novel Hydraulic Hybrid Architecture for On-Road Vehicles. The 13th Scandinavian International Conference on Fluid Power, SICFP2013, June 3-5, 2013, Linkoping, Sweden. ISBN 978-91-7519-572-8.
16. JCMAS H020:2007. Earth-moving machinery – Fuel consumption on hydraulic excavator – Test Procedure.
17. M. Inderelst. Energy improvements in mobile hydraulic systems. Reihe Fluidtechnik. RWTH Aachen University. ISBN: 978-3-8440-1726-7.
18. P. Casoli, A. Anthony, M. Rigosi (2011) "Modeling of an Excavator System – Semi empirical hydraulic pump model" SAE - International Journal of Commercial Vehicles October 2011 vol. 4, Issue 1, pp. 242- 255. ISSN: 1946-391X. doi:10.4271/2011-01-2278. Scopus code: 2-s2.0-84859342015.
19. P. Casoli, N. Pompini, L. Riccò. Simulation of an Excavator Hydraulic System Using Nonlinear Mathematical Models. Journal of Mechanical Engineering (ISSN: 00392480). Under Review.
20. P. Casoli, L. Riccò, C. Dolcin. Modeling and verification of an excavator system –Axial Piston Pump, Kinematics and Load Sensing Flow Sharing Valve Block. Proceeding of the 13th Scandinavian International Conference on Fluid Power, June 3-5, 2013, Linköping, Sweden. http://dx.doi.org/10.3384/ecp1392. ISBN (print): 978-91-7519-572-8.
21. P. Casoli, L. Riccò, F. Campanini, A. Lettini, C. Dolcin (2015) "Mathematical Model of a Hydraulic Excavator for fuel Consumption Predictions" ASME/BATH 2015 Symposium on Fluid Power & Motion Control. Chicago, Illinois, USA, 12-14 October 2015. FPMC2015-9566.
22. P. Casoli, A. Gambarotta, N. Pompini, L. Riccò (2014). Development and application of co-simulation and control-oriented modeling in the improvement of performance and energy saving of mobile machinery., Energy Procedia, Volume 45, 2014, Pages 849–858. Elsevier. http://dx.doi.org/10.1016/j.egypro.2014.01.090. Codice Scopus: 2-s2.0-84893640233.
23. O. Sundstrom, L. Guzzella, "A Generic Dynamic Programming Matlab Function", In Proceedings of the 18th IEEE International Conference on Control Applications, pp. 1625-1630, Saint Petersburg, Russia, 2009.

Supplementary MATLAB .fig files

Click here to download Supplementary MATLAB .fig files: Figure_25.fig

Supplementary MATLAB .fig files

Click here to download Supplementary MATLAB .fig files: Figure_26.fig

Supplementary MATLAB .fig files

Click here to download Supplementary MATLAB .fig files: Figure_27.fig

Supplementary MATLAB .fig files

Click here to download Supplementary MATLAB .fig files: Figure_28.fig

Supplementary MATLAB .fig files

Click here to download Supplementary MATLAB .fig files: Figure_29.fig

Supplementary MATLAB .fig files

Click here to download Supplementary MATLAB .fig files: Figure_31.fig

Supplementary MATLAB .fig files

Click here to download Supplementary MATLAB .fig files: Figure_32.fig

Supplementary MATLAB .fig files

Click here to download Supplementary MATLAB .fig files: Figure_33.fig

Supplementary MATLAB .fig files

Click here to download Supplementary MATLAB .fig files: Figure_30.fig

Supplementary MATLAB .fig files

Click here to download Supplementary MATLAB .fig files: Figure_9.fig

Supplementary MATLAB .fig files

Click here to download Supplementary MATLAB .fig files: Figure_10.fig

Supplementary MATLAB .fig files

Click here to download Supplementary MATLAB .fig files: Figure_11.fig

Supplementary MATLAB .fig files

Click here to download Supplementary MATLAB .fig files: Figure_12.fig

Supplementary MATLAB .fig files

Click here to download Supplementary MATLAB .fig files: Figure_13.fig

Supplementary MATLAB .fig files

Click here to download Supplementary MATLAB .fig files: Figure_14.fig

Supplementary MATLAB .fig files

Click here to download Supplementary MATLAB .fig files: Figure_15.fig

Supplementary MATLAB .fig files

Click here to download Supplementary MATLAB .fig files: Figure_16.fig

Supplementary MATLAB .fig files

Click here to download Supplementary MATLAB .fig files: Figure_18.fig